Normal anatomy of the aqueous humour outflow system in the domestic pig eye

PAUL G. McMENAMIN* AND RAYMOND J. STEPTOE

Department of Anatomy and Human Biology, The University of Western Australia, Nedlands, WA 6009

INTRODUCTION

Investigations of the aqueous humour outflow system (AOS) are prompted by the search for an understanding of the aetiology and pathogenesis of the many forms of glaucoma. One of the factors hindering research in this area is the limited opportunity for the study of normal human tissue. The similarity in morphology of the AOS among simians (Rohen, 1982) has meant that nonhuman simians are considered to be the most pertinent experimental animals. Expense and availability, however, limit the use of these species. Provided care is taken in comparisons, an inexpensive readily available nonsimian species could act as a useful substitute and accelerate the rate at which our understanding of the functional morphology of this system is progressing.

Early comparative anatomical studies of the AOS (Tripathi, 1971, 1974, 1977; Tripathi & Tripathi, 1972) concentrated primarily on the lining of the angular aqueous plexus and no detailed descriptions of the remainder of the drainage tissues in individual nonprimates were reported. Subsequently a variety of nonprimates have been used as animal models in functional studies. These have included hamster (Ohnishi & Tanigushi, 1983), cow (Anderson, Wang & Epstein, 1980), rabbit (Hernandez *et al.* 1983; Grierson *et al.* 1986), cat (Richardson, Marks, Ausprunk & Miller, 1985), rat (McMenamin & Al-Shakarchi, 1989) and dog (Samuelson & Gelatt, 1984*a, b*; Bedford and Grierson, 1986) although detailed morphological data are available for only rabbit, cat, rat, dog and horse (Samuelson, Smith & Brooks, 1989).

In nonsimian mammals which do not possess an accommodatory apparatus, the ciliary body is split into 2 leaves; the outer portion is muscular and lies close to the inner aspect of the sclera, while the inner portion, which may be fibrous or muscular, forms the base plate of the ciliary body and the root of the iris (see Tripathi, 1974, for review). The ciliary cleft, which lies between these 2 portions, is an extension of the anterior chamber. It is crossed by fibrocellular cords or strands which form an angular or reticular meshwork (Tripathi, 1974, 1977). The innermost and largest of the connective tissue cords are the pectinate ligaments which extend from the root of the iris to the inner aspect of the peripheral cornea. The main differences between the primate and nonprimate iridocorneal angle include (1) poorly organised reticular tissue is present in the angle of nonprimates with no clear trabecular or lamellar structures; (2) in nonprimates there is no clear anatomical connection between the ciliary muscle and the drainage tissues; and (3) a single circumferential canal of Schlemm is absent, the canal being represented instead by a series of collector vessels

---

* Corresponding author.

or the angular plexus (AAP) (Tripathi & Tripathi, 1972; Rohen, 1982). The rat, like primates, possesses a single circumferential canal (McMenamin & Al-Shakarchi, 1989); its small size, however, limits it to certain types of studies.

The aim of the present investigation is to provide a detailed description of the morphology of the porcine aqueous outflow system to determine whether it may be a more appropriate model than some of the species currently in use. The pig was specifically chosen because of availability and similar size to the human eye. Surprisingly there have been no previous morphological descriptions of the iridocorneal angle in this species. Comparative anatomical studies may help to explain why the human outflow system is vulnerable to morphological changes associated with the pathogenesis of primary open angle glaucoma.

MATERIALS AND METHODS

Twelve whole eyes were obtained from pigs (from a local abattoir) of live weight greater than 90 kg (age greater than 6 months and less than 2 years). Eight eyes were rapidly enucleated and immersed intact in 2% glutaraldehyde in 0·1 M phosphate buffer immediately after commencement of exsanguination following electrical stunning (total delay of ∼ 2 min). The anterior chamber of a further 2 eyes was cannulated immediately after enucleation and attached via tubing to a reservoir of the same fixative. The eyes were then perfusion fixed for 30 min at 20 mmHg (within the physiological range of most mammals). All eyes were then fixed for a further 24 h and one quadrant was selected randomly from each of 10 eyes so that the complete circumference of the globe would be represented in the samples of tissue processed. Each quadrant was dissected into a number of meridional slices 1–3 mm in thickness. The slices were then processed and embedded in Araldite in the conventional manner. Semithin sections (1–2 μm) were stained with toluidine blue for light microscopy and ultrathin sections (70–90 nm) were taken from selected blocks for transmission electron microscopy. The 20 blocks chosen for study (at least 1 per eye) were sectioned in either meridional or tangential planes. Ultrathin sections were stained with uranyl acetate and counterstained with lead citrate and examined on a Phillips 401 TEM.

To study the circumferential variations in morphology, samples from each quadrant (superior, nasal, inferior and temporal) of a further 2 eyes were processed for both paraffin and resin embedding. Paraffin-embedded tissue was stained by van Gieson and modified van Gieson to investigate the distribution of muscle in the ciliary body. Sections were also stained with Alcian blue involving critical electrolyte concentrations (Scott & Dorling, 1965) to study the distribution of glycosaminoglycans (GAGs) in the anterior segment, particularly the drainage tissues. For scanning electron microscopy one quadrant was taken from each of 3 eyes and dissected into smaller blocks, dehydrated, critical point dried, further dissected if necessary, mounted, sputter-coated with gold and viewed on a Philips 505 SEM.

RESULTS

No notable morphological differences were recorded between eyes fixed by immersion and those fixed by perfusion, with the exception that the latter were marginally better preserved.
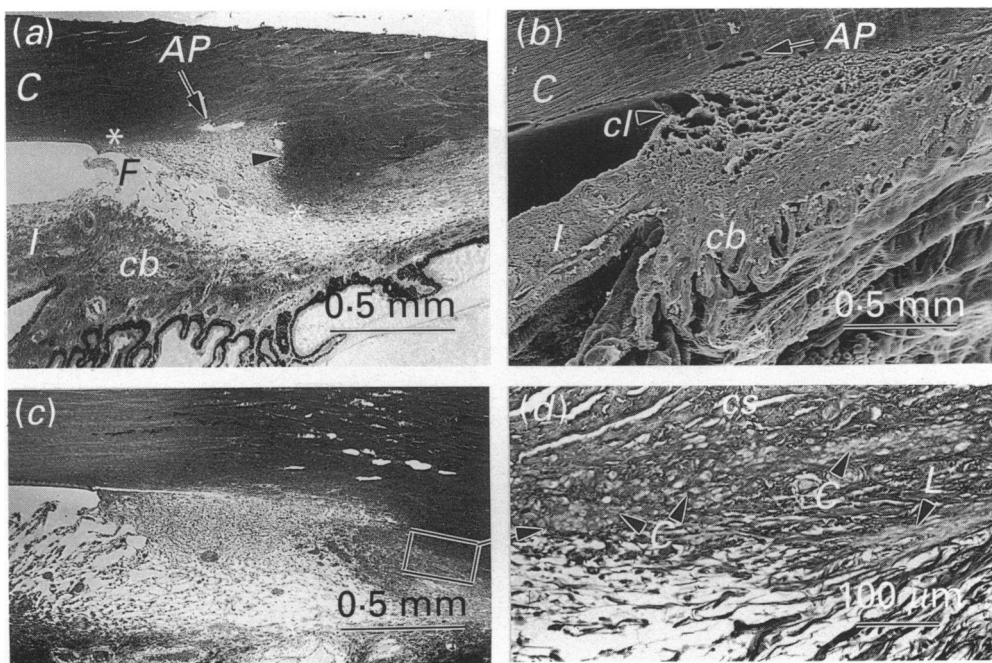
Fig. 1. The porcine iridocorneal angle as seen by LM (*a*, *c*, *d*) and SEM (*b*). (*a*) and (*b*) illustrate the general configuration of the anterior segment in conventional meridional sections. *C*, cornea; *cb*, ciliary body; *I*, iris; *cl*, ciliary cleft; *F*, spaces of Fontana; *AP*, angular aqueous plexus. A line drawn between the 2 asterisks in (*a*) marks the inner limits of the corneoscleral meshwork. (*a*), nasal quadrant, (*c*), temporal quadrant: note the differences in prominence of the 'scleral spur' (▶), the length and volume of the drainage tissue (greater in *c*) and the variation in pigmentation of the pectinate ligaments. (*d*), modified van Gieson from a similar area to that shown in (*c*). Note the longitudinal muscle fibres posteriorly (*L*) and the small ovoid profiles of circumferentially oriented fibres (*C*) close to the dense connective tissue of the corneoscleral junction (cs).

General configuration of the iridocorneal angle and ciliary body

The iridocorneal angle is the extension of the anterior chamber which lies between the iris and the corneoscleral envelope. In the pig, as in most nonprimates, the ciliary body is split into 2 portions by the ciliary cleft (Fig. 1*a–c*). The inner (stromal) portion of the ciliary body is composed of richly vascularised and innervated connective tissue stroma containing a few melanocytes, lined internally by a double layer of pigmented and nonpigmented ciliary epithelium (Fig. 1*a*, *b*). The anterior portion (pars plicata) consists of characteristic radially arranged ciliary processes. The anterior-most or iridial ciliary processes are long and delicate in nature (Fig. 1*a*, *b*). The outer (scleral) portion of the ciliary body consists of a few bands of ciliary smooth muscle fibres embedded in relatively dense irregular connective tissue close to the sclera (Fig. 1*d*). The ciliary muscle in all sections appears to contain an anterior portion in which the fibres are circumferentially oriented in small discontinuous bundles or individual fibres, and a posterior portion in which the fibres have a meridional or longitudinal orientation (Fig. 1*d*).

The ciliary cleft extends approximately 1·5 mm into the ciliary body (Fig. 1*a*, *b*) and is 0·3–0·4 mm at its widest point (anteriorly) where it consists of the large spaces of Fontana, delineated anteriorly by stout pectinate ligaments (PL). The posterior portion of the cleft is crossed by the less robust uveal cords. (Fig. 1*a–c*). There is a
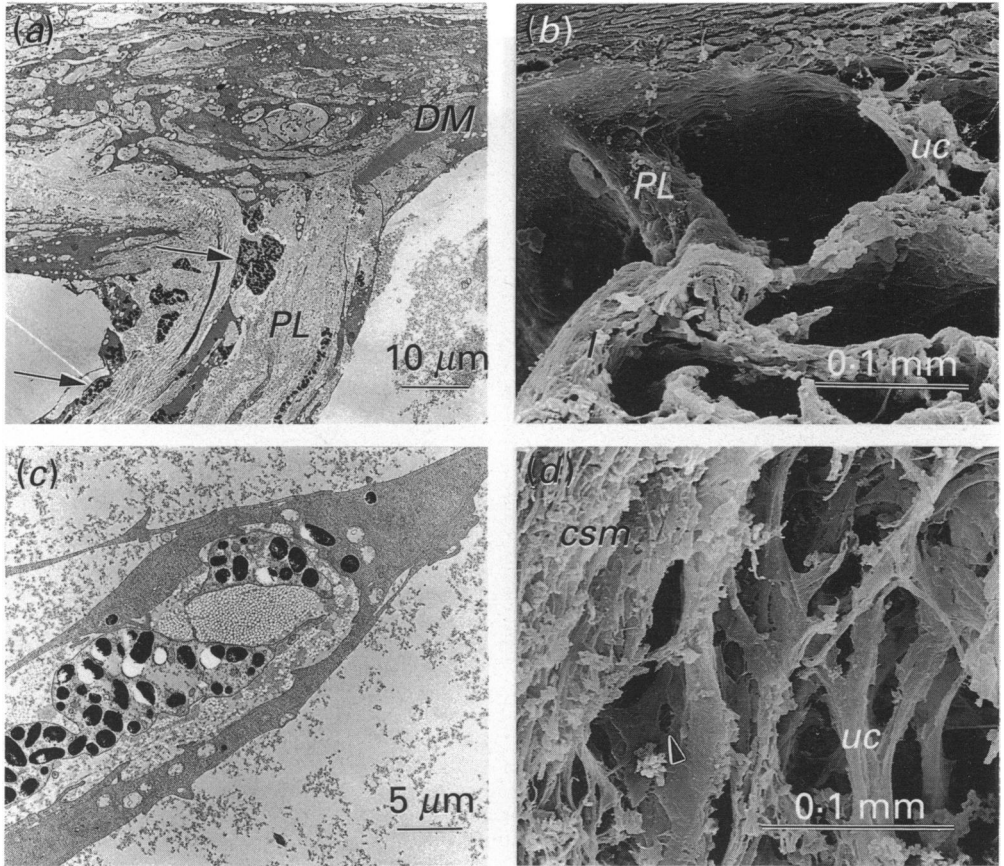
Fig. 2. Medium power TEM and SEM illustrating the morphology of the pectinate ligaments (*PL*) which merge with the corneal stroma and Descemet's membrane (*DM*) on one side of the ciliary cleft and the iris (*I*) on the other. Note the numerous melanocytes (↘) in (*a*) and the innermost robust uveal cords (*uc*) in (*b*), TEM of the uveal cords in (*c*) shows that they consist of endothelial cells enclosing melanocytes and a less substantial collagenous core than pectinate ligaments. (*d*), SEM of tangentially cut specimen reveals the abrupt transition between uveal cords and corneoscleral trabeculae (*csm*). An ovoid intratrabecular space is evident (▶).

distinct internal scleral sulcus which houses the compact corneoscleral meshwork, tissue analogous to the cribriform layer, and the AAP. The posterior lip of this sulcus resembles the 'scleral spur' of primates (Fig. 1*a*).

Circumferential variation

One of the most conspicuous variations around the circumference of the limbus is the depth of the internal scleral sulcus (i.e. the prominence of the 'scleral spur') which houses the meshwork tissue. This sulcus is most evident in the nasal (Fig. 1*a*) and inferior quadrants, but barely distinguishable in the other quadrants (Fig. 1*c*). Consequently there are major variations in the configuration and size of the trabecular tissue; there is, for example, a larger volume of drainage tissue in the temporal and superior quadrants (Fig. 1*c*). The meridional ciliary muscle fibres are slightly larger in the superior and inferior quadrants, but there is no particular variation in the few circularly oriented fibres. The pectinate ligaments are more robust in the nasal and temporal quadrants and pigmentation varies slightly around the circumference.
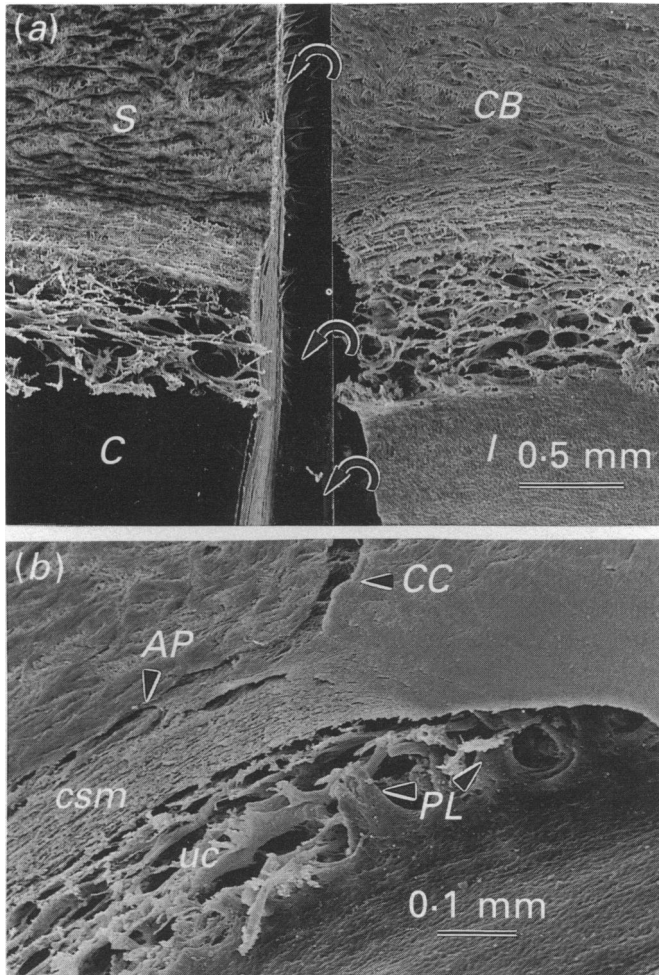
Fig. 3. SEMs of specimens which have been split tangentially through the angular meshwork to display the 3-dimensional arrangement of the trabeculae and spaces. The 2 separate parts in (*a*) are the opposing cut surfaces from one specimen which has been divided in the plane of the ciliary cleft—in the left portion part of the meshwork has been retained with the cornea (*C*) and sclera (*S*) while the portion on the right also contains some meshwork tissue together with the iris (*I*) and ciliary body (*CB*). Note the orientation of the uveal meshwork fibres and gradual diminution in size of the intertrabecular spaces deeper in the cleft. (*b*), another piece of tissue prepared similarly to (*a*), but cut in a more oblique plane, to illustrate the pectinate ligaments (*PL*), uveal cords (*uc*), corneoscleral meshwork (*csm*), vessels of the angular aqueous plexus (*AP*) and a draining collector channel (*CC*).

Pectinate ligaments and uveal cords

The pectinate ligaments, which bridge the ciliary cleft anteriorly from the root of the iris to the posterior margin of Descemet's membrane in the peripheral cornea, are up to 50–60 μm in thickness (Figs 2*a*, *b*, 3*b*). They consist of a well developed core of collagen fibres in which numerous fibroblasts and melanocytes are embedded (Fig. 2*a*). This core is completely enclosed by endothelial cells which possess small cytoplasmic processes or pegs that extend through the basal lamina into the collagenous matrix of the pectinate ligaments (not shown). Near their origin on the cornea there is a slight extension of Descemet's membrane into the ligaments (Fig. 2*a*).
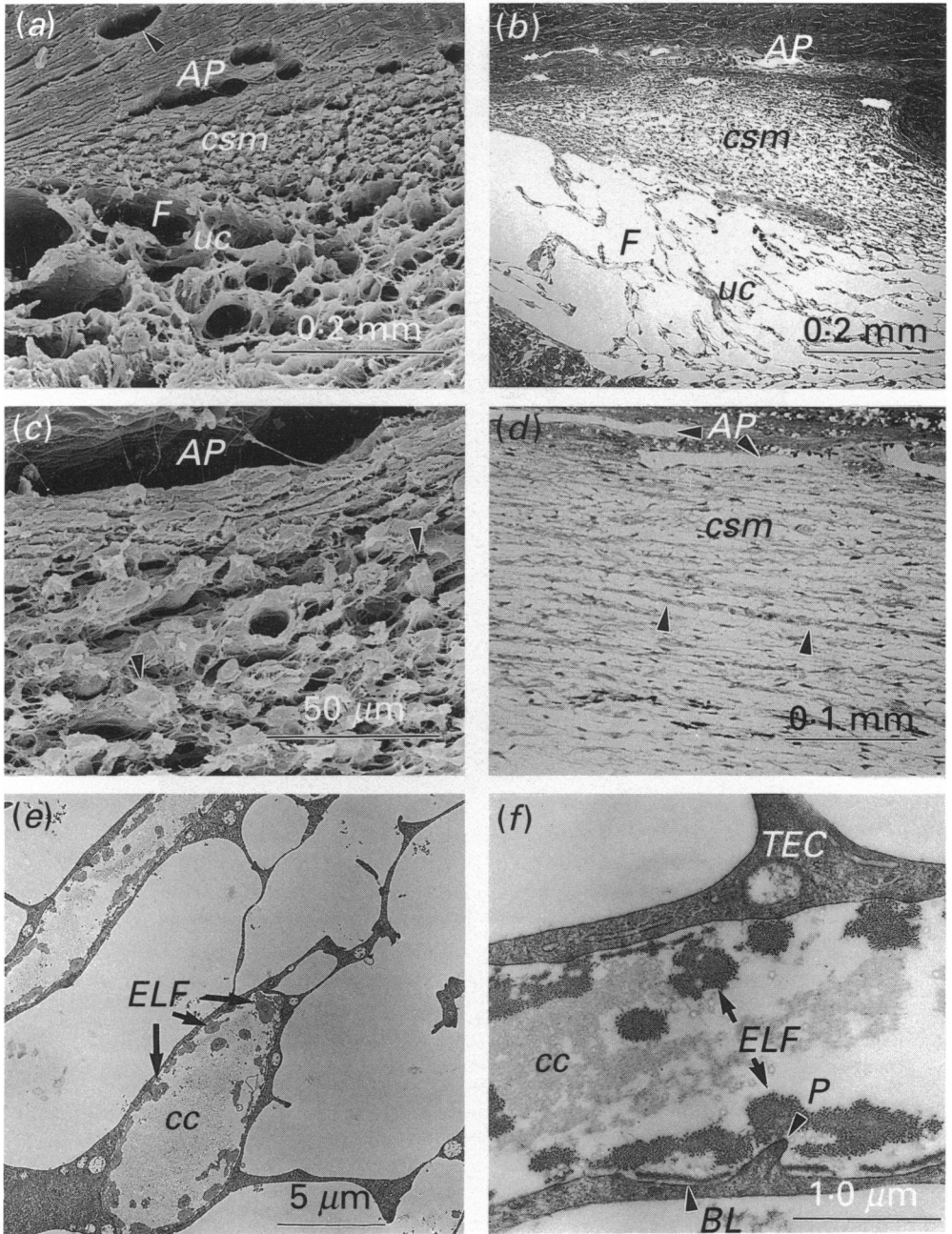
Fig. 4. SEMs (*a, c*), LMs (*b, d*) and TEMs (*e, f*) of the pig trabecular meshwork. (*a–c*) are conventional meridional sections, (*d*) is a tangential or coronal section parallel to the equator. Both orientations reveal the nature of the uveal cords (*uc*), spaces of Fontana (*F*), corneoscleral meshwork (*csm*) and vessels of the angular aqueous plexus (*AP*). At higher magnification the corneoscleral trabeculae are seen as round or ovoid profiles in meridional sections but appear as elongated fibres in tangential sections (▶) in (*d*), (*e*) and (*f*), low and high power of well organised trabeculae in the corneoscleral meshwork. Note the arrangement of the collagen fibres in the core (*cc*), the elastic-like fibres (*ELF*) in the cortical region, basal lamina (*BL*) beneath the covering of TECs some of which exhibit peg-like extensions (*P*). A collector channel is indicated in (*a*) (▶).
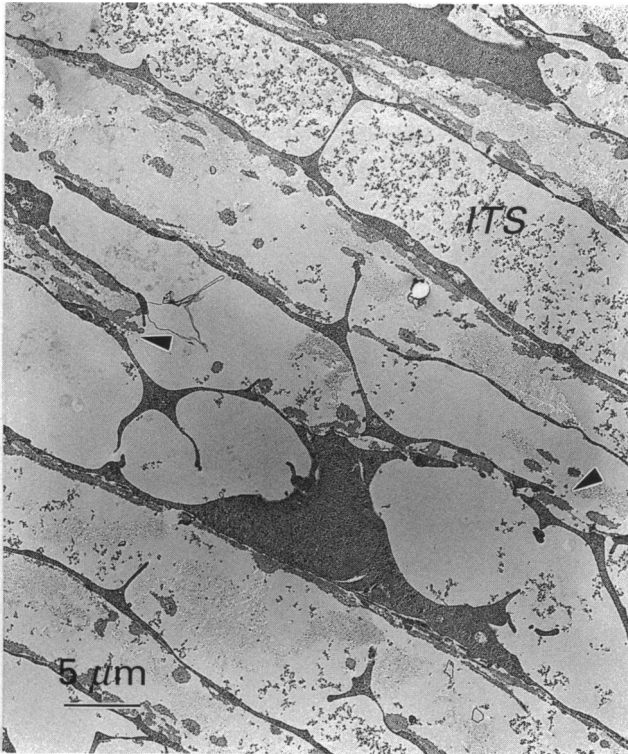
Fig. 5. TEM of the outer corneoscleral meshwork to illustrate the partly incomplete cover of TECs evident in some areas (▶). Note the flocculent or plasmoid material in the intertrabecular spaces (*ITS*).

There is a gradual transition in thickness and organisation of the uveal cords from anterior to posterior, i.e. those located anteriorly are thicker ($\sim 20 \mu$m) with a well developed fibrous core (Fig. 2b) whilst those deeper in the ciliary cleft are composed of loosely arranged collagen fibres enveloped by endothelial cells (Fig. 2c). Melanocyte processes and elastic-like fibres are also occasionally present within the innermost uveal cords (Fig. 1e). The endothelial lining of some uveal cords is incomplete; the matrix is thus exposed to the aqueous humour in the intertrabecular spaces (ITS) (not illustrated). Where the endothelial cells are closely apposed to the collagen core a thin incomplete layer of basal lamina intervenes. These uveal cords at first appear to be randomly oriented as incomplete perforated sheets or as a series of fine cords with variable sized ITS or gaps (Fig. 2d). Scrutiny of tangentially divided specimens reveals the predominantly circumferential nature of the uveal cords (Figs 2d, 3a, b). The endothelial cells of the uveal cords have a large number of fine cytoplasmic processes of sheet-like extensions which further subdivide the inter and intratrabecular spaces.

Corneoscleral meshwork (CSM)

A sharp delineation, evident by both LM and SEM in meridional sections, occurs in the arrangement of the meshwork tissue close to the sclera (Figs 1a–c, 4a, b). The open-meshed uveal cords of the ciliary cleft are replaced by a wedge-shaped mass of tightly compacted trabeculae which fills the internal scleral sulcus (Fig. 1a, b). The line of delineation extends from the equivalent of Schwalbe's line to a point on the sclera

similar to the scleral spur (asterisks in Fig. 1 *a*). This delineation, however, is even more clearly demonstrated in tangential slices viewed by SEM (Figs 2*d*, 3*a*, *b*). The shape and orientation of the trabeculae are slightly different from the lamellate form present in primates in that they appear as ovoid profiles in conventional sections (Fig. 4*a–c*) while appearing elongated in the circumferential plane in tangential sections (Fig. 4*d*). Often the trabeculae are completely covered by trabecular endothelial cells (TECs) (Figs 4*e,f*, 5), although in a few areas the cores are apparently open to the intertrabecular spaces (arrows in Fig. 5). Beneath the endothelial cells an incomplete basal lamina, thicker than in the uveal cords, can be identified (Fig. 4*f*). Bundles of elastic-like fibres, consisting of a condensed electron lucent core and fibrillar exterior, are arranged circumferentially within the cortical zone of the trabeculae and also to a much lesser extent within the collagenous core (Figs 4*e,f*, 5). No plaques of long spacing collagen, which occur in the cortical zone of human trabeculae (McMenamin, Lee & Aitken, 1986), are evident in the porcine trabeculae. The TECs contain only a few organelles, chiefly located in the perikaryon (Fig. 4*e, f*). Numerous cell processes, evident by both LM and SEM, radiate from the trabeculae, thus subdividing the ITS (Figs 4*c, e*, 5).

One feature found in some blocks, from both perfusion and immersion fixed eyes, was the presence of loose flocculent or plasmoid material in the ITS of the CSM and the spaces of Fontana (Figs 2*a, c*, 5). This material was initially suspected to be GAGs but Alcian blue staining at critical electrolyte concentrations revealed no staining in the ITS.

Large myelinated and unmyelinated nerves were frequently noted in the corneoscleral and uveal meshworks.

Cribriform layer of juxtacanalicular zone

Beneath the lining endothelium of the AAP a thin zone exists which is morphologically analogous to the cribriform layer of primates; i.e. TECs are surrounded by various types of extracellular matrix and apparently electron lucent spaces (Fig. 6*a, b*). There is no lamellate or trabecular arrangement in this zone. Where there are no AAP vessels the CSM merges with the dense connective tissue of the corneoscleral sulcus (Fig. 6*a*). Fine collagen fibres, elastic-like fibres and a small amount of fine fibrillar material are interspersed amongst the large extracellular spaces. A noticeable basal lamina surrounds many of the cells in this region and is also present on the abluminal aspect of a large proportion of the lining endothelium of the AAP, even beneath 'giant vacuoles' (Fig. 6*c*). In areas adjacent to collector channels (see below) there was occasionally herniation of the loose cribriform tissue into the ostia of these drainage vessels (not illustrated).

The angular aqueous plexus (AAP)

The AAP is made up of the number of endothelial-lined canals or vessels lying between the dense connective tissue of the corneoscleral junction on their outer aspect and the trabecular meshwork on their inner aspect (Figs 1*a, b, c*, 4*a, b, d*). Occasionally small canals are seen completely surrounded by meshwork-like tissue, i.e. lacking a dense outer wall. These are most likely inner diverticulae of the main vessels. The lumina of the AAP are frequently septate (Figs 2*b*, 3*a, b, d*). The septae range from long slender bridges to more sheet-like structures. The endothelial cells lining these canals have their long axis in the circumferential plane (not illustrated) similar to primates. The lining endothelium of the AAP is characterised by giant vacuoles, 3–10 μm in diameter (Fig. 6*a, c*). Pore-like structures are present on the abluminal or
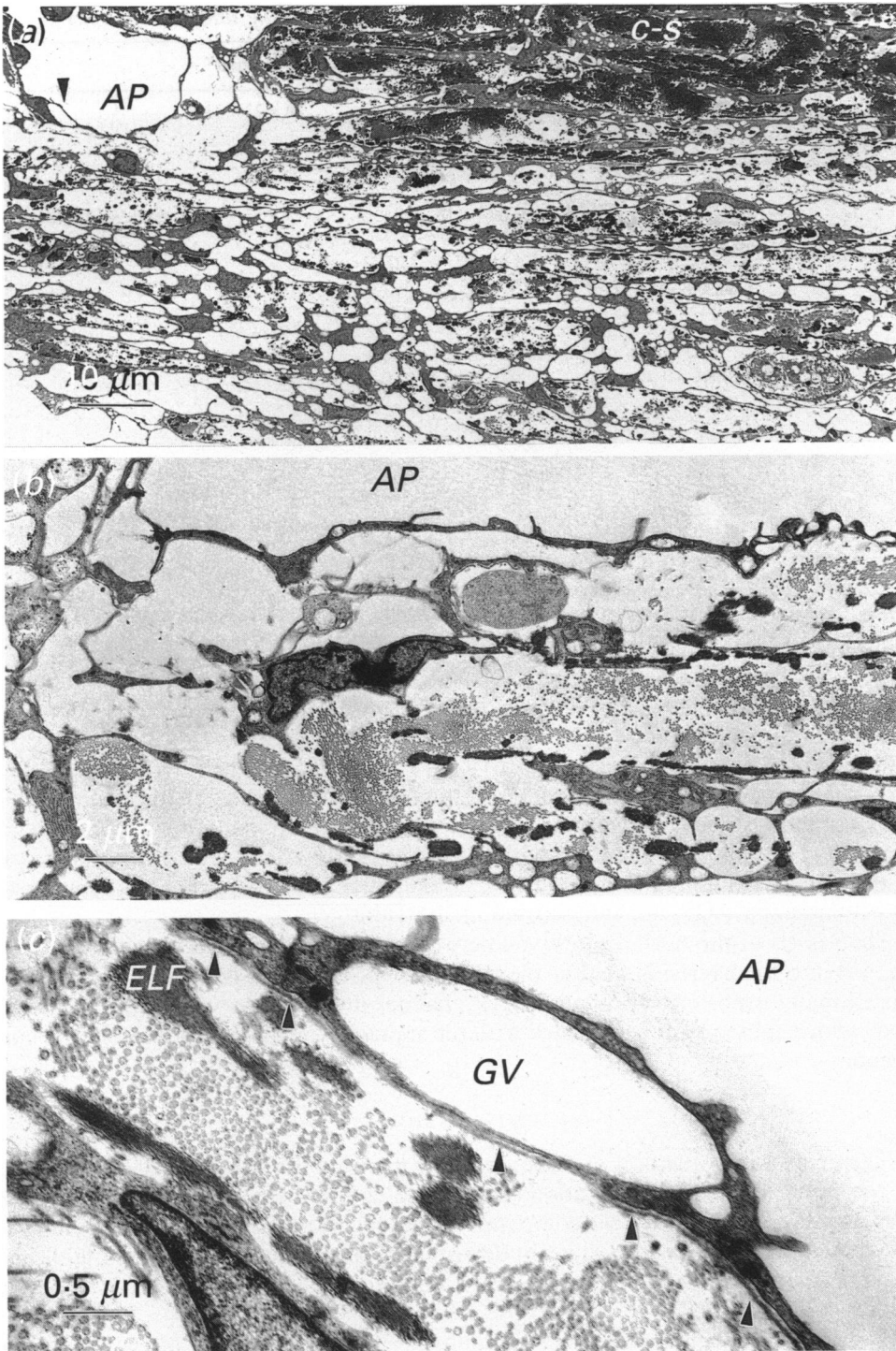
Fig. 6. TEMs of the outer meshwork or cribriform layer adjacent to the angular aqueous vessels (*AP*) and the dense connective tissue of the corneoscleral junction (*C–S*). Note the large electron lucent spaces around the angular aqueous vessel in (*a*) and at higher magnification in (*b*). A single giant vacuole (▶) is indicated in (*a*) and another (*GV*) is seen in more detail in (*c*). Note the large quantities of rough endoplasmic reticulum in the cells of the outer meshwork in (*b*). The basal lamina material (▶) beneath the lining endothelium of the angular aqueous vessel is evident in (*c*).

Table. *Comparison of dimensions between the porcine and human eyes*

	Pig[a]	Human[b]
Globe size (mm) [±SD]	20·1 × 23·5 × 24·9 [0·74] [0·85] [0·87]	24 × 23 × 23·5
Globe weight (g)	—	6·7–7·5
Globe volume (ml) [±SD]	6·5 [0·3]	6·5
Anterior chamber volume (ml)	300	300
Volume of trabecular tissue (μl)	19·8* [4·45]	4·5
No of AAP vessels n = 10 [±SD]	4·8 [0·85]	Canal of Schlemm (often septate)
Size of AAP vessels (μm) (depth × length)** n = 10	5–30 × 15–150	10–25 × 200–400

[a] Based on measurements made by the authors, n = 7. Globe volume measured by water displacement.
[b] Based on various sources in literature (Spector, 1956; Wolff, 1961; Jakobiec & Ozanics, 1982).
* Whole ciliary cleft, figures in parentheses represent the volume of corneoscleral tissue in the scleral sulcus (see Fig. 1).
** Assessed in 1 semithin section per block. Measurements are in ranges.

trabecular aspect of the giant vacuoles. No pores were seen on the luminal aspect in the sections examined; however no serial sections were prepared. The number and size of vessels or canals which constitute the AAP varies. Results of a quantitative analysis of these vessels and other morphometric measurements, with appropriate comparison with the human AOS, are summarised in the Table.

The vessels of the AAP drain by numerous interconnected collector channels (Figs 3b, 4b) into the overlying venous plexus of the episclera and peripheral conjunctiva. Occasionally a posteriorly-located AAP channel drained into venules in the ciliary body which subsequently connected with the suprachoroidal/choroidal vortex venous system.

DISCUSSION

The present investigation was prompted by the need for a more precise knowledge of the outflow systems of additional nonprimates than is currently available in the literature. Precise details of the comparative anatomical and ultrastructural differences and similarities may be important in determining the relative value and suitability of any one species for in vivo and in vitro studies and as animal models of the human outflow system.

The pig outflow system in general conforms to the pattern of other nonprimate mammalian species. For example, in the pig the ciliary cleft is bridged anteriorly by robust pectinate ligaments which precede fine uveal cords, both of which form the uveal or iridocorneal meshwork, a pattern common in other nonprimates (Tripathi, 1971, 1974, 1977; Tripathi & Tripathi, 1972) including the dog (Samuelson & Gelatt,

1984*a*, *b*; Bedford & Grierson, 1986), cat (Richardson *et al.* 1985), and horse (Samuelson *et al.* 1989). However, it appears that in the pig the triangular wedge of corneoscleral trabecular tissue, lying within the shallow scleral sulcus, has more features in common with the primate system such as size, shape (Table) and lamellar architecture than other species. Furthermore, the volume and size of the eye, and in particular the anterior chamber, is closer to the human than any other species reported (Table). These macroanatomical features alone would suggest that it may be a valuable species as a source of tissue for in vitro or whole anterior chamber organ culture studies (Johnson & Tschumper, 1987) or laser trabeculotomy and trabeculectomy studies.

In the pig the corneoscleral trabeculae are well organised and less reticular in nature than in other species. The trabeculae consist of the usual components, a collagenous core surrounded by a cortical zone which contains elastic-like fibres, both ensheathed by TECs and their incomplete basal laminae. Differences from human trabeculae include the partially incomplete cellular cover, the interrupted basal lamina, and the lack of deposition of long-spacing collagen and extracellular components in the cortical zone. This absence of material in the cortical region may be due to the relatively young age of the animals studied since this is a well recognised age-related phenomenon (Rohen & Lutjen-Drecoll, 1971; McMenamin *et al.* 1986, and others). The TECs in the pig possess numerous delicate cytoplasmic extensions which further subdivide the intertrabecular spaces, a pattern more analogous to that observed in the human fetal eye than in the adult (Reme & Lalive d'Epinay, 1981; McMenamin, 1991). Whilst some degree of TEC detachment from the connective tissue matrix may be an artefact resulting from the processing of such delicate tissue, the consistent nature of this feature and the lack of any other artefactual changes are compelling evidence that some incomplete cellular cover is a feature of this species.

The flocculent material in the intertrabecular spaces of some specimens was not Alcian blue positive and is most likely plasma which had leaked from iris vessels, possibly as a result of localised breakdown of the blood–ocular barrier at the time of death.

The configuration of the ciliary muscle and ciliary body appears to be an important determining factor in the overall arrangement of the iridocorneal angle in mammals. In general the muscle is poorly developed in herbivores, consisting only of meridionally oriented fibres that provide little structural support for the iris base. In primates a large complex ciliary body musculature has evolved as part of the accommodation apparatus. The carnivores, including the cat (Richardson *et al.* 1985), dog (Samuelson & Gelatt, 1984*a*, *b*; Bedford & Grierson, 1986) and racoon (Rohen *et al.* 1989) are intermediate and possess a moderately well developed musculature of meridional and radial fibres. In the pig the ciliary body appears to contain a mixture of both meridional and circumferential muscle fibres. Rohen (1982) has stated that only longitudinally oriented fibres occur in nonprimates. However, there have been several reports in the literature of variable amounts of smooth muscle fibres close to the aqueous outflow pathways of the rabbit (Knepper, Farbman & Bondareff, 1975) and rat (Tsukahara, 1978; McMenamin & Al-Shakarchi, 1989), especially close to the angular aqueous vessels. Whether such smooth muscle fibres are of functional significance in these species and possibly in the pig is uncertain at this time.

Loose cribriform tissue often appeared to herniate into the vessels of the AAP and their diverticulae. This is an appearance most commonly found in nonprimates, e.g. dogs (Bedford & Grierson, 1986), but may also occur in primates after prolonged perfusion (McMenamin & Lee, 1986) or at elevated intraocular pressure (Grierson &

Lee, 1974). This particular appearance is similar to that found in the brain where the arachnoid villi pierce the dense connective tissue of the dura mater, which are the respective anatomical analogues of the trabecular meshwork and Schlemm's canal.

In summary, this study describes the anatomical and ultrastructural features of the aqueous outflow pathways in the domestic pig. It would appear, provided certain dissimilarities to the primate aqueous outflow system are kept in mind, that this particular species may be one of the most suitable and readily available species for investigations into the functional morphology of the aqueous outflow pathways.

SUMMARY

The normal functional anatomy of the aqueous humour outflow pathways in the domestic pig is poorly documented in the literature despite its being readily available and of a similar size to the human eye. Anterior segment tissue from 12 pig eyes was appropriately fixed and investigated by light microscopy, and scanning and transmission electron microscopy. The configuration of the iridocorneal angle tissues is similar to other nonprimate mammals in several respects, i.e. it possesses a deep ciliary cleft crossed by stout pectinate ligaments and delicate uveal cords, poorly developed ciliary musculature, and an angular aqueous plexus. However, there were some noteworthy features which may make it a suitable model for specific types of glaucoma related research. These features include a shallow scleral sulcus which contains a wedge-shaped mass of corneoscleral tissue comparable in size to the human trabecular meshwork. This tissue was more trabecular than 'reticular' in arrangement, the latter being the more common in nonprimate mammalian species. The relevance of the present findings to the use and limitations of the porcine eye as a model of the human aqueous outflow pathways is discussed.

REFERENCES

ANDERSON, P. J., WANG, J. & EPSTEIN, D. L. (1980). Metabolism of calf trabecular (reticular) meshwork. *Investigative Ophthalmology and Visual Science* **19**, 13–20.

BEDFORD, P. G. C. & GRIERSON, I. (1986). Aqueous drainage in the dog. *Research in Veterinary Science* **41**, 172–186.

GRIERSON, I. & LEE, W. R. (1974). Changes in the monkey outflow apparatus at graded levels of intraocular pressure: a qualitative analysis by light microscopy and scanning electron microscopy. *Experimental Eye Research* **19**, 21–33.

GRIERSON, I., NAGASUBRAMANIAN, S., EDWARDS, J., MILLAR, L. C. & ENNIS, K. (1986). The effects of various levels of intraocular pressure on the rabbit's outflow system. *Experimental Eye Research* **42**, 383–397.

HERNANDEZ, M. R., WEINSTEIN, B. I., WENK, E. J., GORDON, G. G., DUNN, M. W. & SOUTHERN, A. L. (1983) The effect of dexamethasone on the in vitro incorporation of precursors of extracellular matrix components in the outflow pathway region of the rabbit eye. *Investigative Ophthalmology and Visual Science* **24**, 704–709.

JAKOBIEC, F. A. & OZANICS, V. (1982). General topographic anatomy of the eye. In *Ocular Anatomy, Embryology and Teratology* (ed. F. A. Jakobiec), pp. 1–9. Philadelphia: Harper & Row.

JOHNSON, D. R. & TSCHUMPER, R. C. (1987). Human trabecular meshwork organ culture. *Investigative Ophthalmology and Visual Science* **28**, 945–953.

KNEPPER, P. A., FARBMAN, A. I. & BONDAREFF, W. (1975). A smooth muscle plexus associated with the aqueous outflow pathway of the rabbit eye. *Anatomical Record* **182** 41–52.

MCMENAMIN, P. G. (1991). Quantitative studies of the prenatal development of the human outflow system. *Experimental Eye Research*, in press.

MCMENAMIN, P. G. & LEE, W. R. (1986). Effects of prolonged intracameral perfusion with mock aqueous humour on the morphology of the primate outflow apparatus, *Experimental Eye Research* **43**, 129–141.

MCMENAMIN, P. G., LEE, W. R. & AITKEN, D. A. N. (1986). Age-related changes in the human outflow apparatus *Ophthalmology* **93**, 194–208.

MCMENAMIN, P. G. & AL-SHAKARCHI, M. J. (1989). The effect of various levels of intraocular pressure on the rat aqueous outflow system. *Journal of Anatomy* **162**, 67–82.

OHNISHI, Y. & TANIGUSHI, Y. (1983). Distribution of ^{35}S-sulfate and ^{3}H-glucosamine in the angular region of the hamster: light and electron microscopic autoradiography. *Investigative Ophthalmology and Visual Science* **24** 697–703.

REME, C. & LALIVE D'EPINAY, S. (1981). Periods of development of the normal human chamber angle. *Documenta Ophthalmologica* **51**, 241–268.

RICHARDSON, T. M., MARKS, M. S., AUSPRUNK, D. H. & MILLER, M. (1985). A morphologic and morphometric analysis of the aqueous outflow system in the developing cat eye. *Experimental Eye Research* **41**, 31–51.

ROHEN, J. W. (1982). The evolution of the primate eye in relation to the problem of glaucoma. In *Basic Aspects of Glaucoma Research* (ed. E. Lutjen-Drecoll), pp. 3–33. Stuttgart: Schattauer.

ROHEN, J. W. & LUTJEN-DRECOLL, E. (1971). Age changes of the trabecular meshwork in the human and monkey eyes. In *Age Changes in the Eye (Altern und Entwicklung)* (ed. H. Bredt & J. W. Rohen), pp. 1–36. Stuttgart: Schattauer.

ROHEN, J. W., KAUFMAN, P. L., EICHORN, M., GOECKNER, P. A. & BITO, L. (1989). Functional morphology of accommodation in the racoon. *Experimental Eye Research* **48**, 523–537.

SAMUELSON, D. A. & GELATT, K. N. (1984a). Aqueous outflow in the beagle. I. Postnatal morphological development of the iridocorneal angle: pectinate ligament and uveal trabecular meshwork. *Current Eye Research* **3**, 783–794.

SAMUELSON, D. A. & GELATT, K. N. (1984b). Aqueous outflow in the beagle. II. Postnatal morphological development of the iridocorneal angle: the corneoscleral trabecular meshwork and angular aqueous plexus. *Current Eye Research* **3**, 795–807.

SAMUELSON, D. A., SMITH, P., BROOKS, D. (1989). Morphologic features of the aqueous humor drainage pathways in horses. *American Journal of Veterinary Research* **50**, 720–727.

SCOTT, J. E. & DORLING, J. (1965). Differential staining of acid glycosaminoglycans (mucopolysaccharides) by Alcian blue in salt solutions, *Histochemie* **5**, 221–233.

SPECTOR, W. (ed.) (1956). *Handbook of Biological Data*, pp. 290. Philadelphia: W. B. Saunders.

TRIPATHI, R. C. (1971). Ultrastructure of the exit pathway of the aqueous in lower mammals. *Experimental Eye Research* **12**, 311–344.

TRIPATHI, R. C. (1974). Comparative physiology and anatomy of the aqueous outflow pathway. In *The Eye*, vol. 5 (ed. H. Davson), pp. 163–356. London: Academic Press.

TRIPATHI, R. C. (1977). The functional morphology of the outflow systems of ocular and cerebrospinal fluids. In *The Ocular and Cerebrospinal Fluids* (ed. L. Z. Bito, H. Davson & J. D. Fenstermacher), pp. 65–116. London: Academic Press.

TRIPATHI, R. C. & TRIPATHI, B. J. (1972). The mechanism of aqueous outflow in lower mammals. *Experimental Eye Research* **14**, 73–79.

TSUKAHARA, S. (1978). The existence of smooth muscle adjacent to the Schlemm's canal of the normal albino rat eye. *Acta ophthalmologica* **56**, 735–741.

WOLFF, E. (1961). *The Anatomy of the Eye and Orbit*, p. 30. London: H. K. Lewis.